DOI: 10.1002/chem.201101005

Self-Organizing Domino-Like Superlattices through Stereochemical Recognition Match at the Organic–Inorganic Interface in Solution

An-Xiang Yin, Ya-Wen Zhang,* and Chun-Hua Yan*[a]

Nature produces various self-assembled architectures of different scales and with unique functions spontaneously through delicate control of building blocks at a molecular level.[1–2] In the laboratory, chemical self-assembly of molecules or nanocrystals is considered to be one of the most practical approaches to build up various functional nanostructures, as well as plenty of potential nanodevices through the "bottom-up" approach.[3] Many unique collective properties could be realized by the self-assembly of various nano building blocks with different symmetries into ordered superstructures.[4–10]

General principles of self-assembly can be summarized in two rules: 1) Like prefers like, and 2) self-assembly is driven by total energy minimization.[3] Further studies on natural biological superstructures or functional minerals[2] reveal that local stereochemical recognition at the organic–inorganic interface plays an important role in the formation of self-assembled organic–inorganic hybrid structures, directed by specific macromolecules with specialized stereochemical configurations. Hybrid superstructures self-assemble spontaneously through the cooperation and recognition of both organic and inorganic species at the organic–inorganic interface. In contrast, present trials for chemical self-assembly of nanocrystals are rigid and tedious. Commonly employed methods are "post-synthesis" assembly procedures, in which external forces are still needed to form the assembled structures through usual procedures, such as evaporation-induced self-assembly (EISA) and Langmuir–Blodgett (LB) compressing,[5,11–13] instead of a simultaneous and spontaneous route. The key factors considered in these procedures are mainly focused on the level of "particle", such as the size (several nanometers), shape, and electrostatic properties of the nanocrystals.[5,12] While the stereochemical recognition of the capping surfactant molecules at the molecular level (several hundred picometers), as well as their configurations at the organic–inorganic interface, are still not well understood, although it has been proved to be a fundamental factor for the spontaneous self-assembly in biochemical or biomimetic systems[14–16] and might also play an important role in the spontaneous self-assembly of nanocrystals in solutions.[17–19]

As is known, alkaline earth halides are widely used in optoelectronic and microelectronic devices[20] or photostimulated luminescence storage devices.[21] Here, we demonstrate the wet-chemical preparation of close-packed and ordered-aligned, luminescent, domino-like superlattices of ultrathin nanoplates of alkaline earth halides (BaFCl, SrFCl, BaFBr). Assisted by a molecular mechanics simulation, the stereochemical recognition match of different chemical species (mainly alkaline earth cations and long-chain surfactants) at the organic–inorganic interface is ascribed to be the decisive factor for the solution-based spontaneous self-assembly of the nanoplate superlattices. The as-formed micelle structure of long-chain surfactant molecules of oleic acid (OA) and oleylamine (OM) acts as both the shape-directing agent (ShDA)[22] for the ultrathin nanoplates and the structure-directing agent (StDA)[23,24] for the self-assembled 1D superlattices.

Structures and compositions of the self-assembled domino-like superlattices were confirmed by means of transmission electron microscopy (TEM), high-resolution TEM (HRTEM), energy dispersive X-ray spectroscopy (EDS) analysis, and X-ray diffraction (XRD) measurements. TEM images (Figure 1 and Figure S1 in the Supporting Information) reveal that these highly compact and ordered superlattices (SP) of ultrathin BaFCl nanoplates, obtained from face-to-face formation, can reach a length of tens of micrometers or even longer. These uniform rectangular nanoplates have a thickness of (2.3 ± 0.4) nm and an edge length of (79.8 ± 4.5) nm. Interestingly, the interplate distances are generally no more than 2 nm (Figure 1 and Figure S2 in the Supporting Information), fitting the thickness of only one monolayer of the OA/OM molecules and thus suggesting that a penetrating stereostructure would be adopted by these interplate surface ligands. HRTEM images (Figure 1d and f) show that these uniform nanoplates, preferring to grow faster along the $<100>$ direction, are single crystals bound by (110), $(\bar{1}10)$ and (001) facets, and that they tend to

[a] A.-X. Yin, Prof. Y.-W. Zhang, Prof. C.-H. Yan
Beijing National Laboratory for Molecular Sciences
State Key Laboratory of Rare Earth Materials Chemistry and Applications
PKU-HKU Joint Laboratory in Rare Earth Materials and Bioinorganic Chemistry
College of Chemistry and Molecular Engineering
Peking University, Beijing 100871 (P. R. China)
Fax: (+86) 10-6275-4179
E-mail: ywzhang@pku.edu.cn
yan@pku.edu.cn

Supporting information for this article is available on the WWW under http://dx.doi.org/10.1002/chem.201101005.

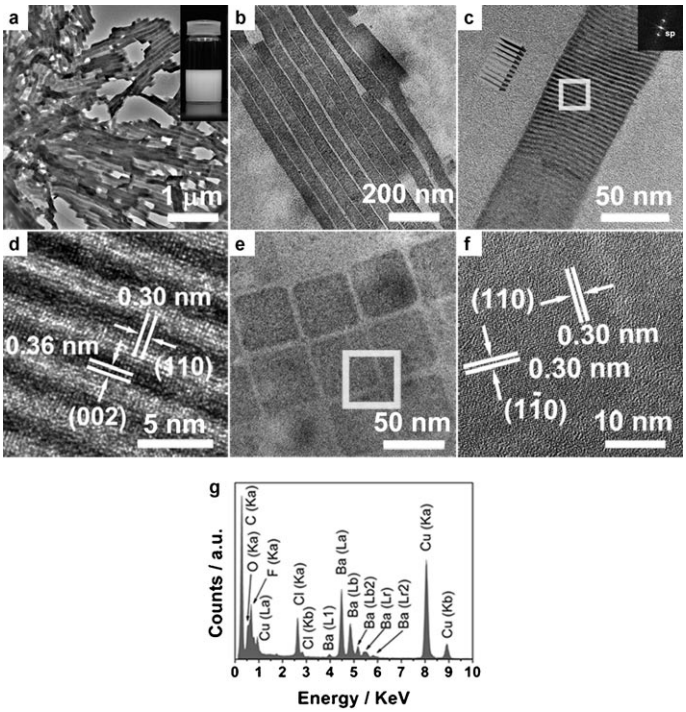

Figure 1. TEM images and EDS characterization of superlattices of ultrathin BaFCl nanoplates. a)–c) TEM images of the self-assembled superstructures of ultrathin BaFCl nanoplates [Inset in panel a): a digital image of the gel-like dispersion of the nanoplates; insets in panel c): a structural model of the nanoplate array and FFT pattern]. d) HRTEM images of BaFCl nanoplates highlighted in panel c) with the square. e) TEM image of separated single-layered nanoplates. f) HRTEM image of BaFCl nanoplates highlighted in panel e) with the square. g) The corresponding EDS spectrum of the nanoplates depicted in panel b).

self-assemble along the $<001>$ direction into layered mesostructures. EDS analysis indicates that these self-assembled nanoplates mainly contain elements of barium, fluorine, chlorine, and oxygen at an atomic ratio of 30.0:28.7:20.5:11.8 (Figure 1g), suggesting the probable replacement of halogen anions (especially Cl^- ions) by carboxyl species at the organic–inorganic interface, that is, at both the upper and bottom (001) facets of each single nanoplate. This replacement of Cl^- species by carboxyl groups is favored energetically by comparison of the bond energy of Ba–F (136 kcal mol^{-1}), Ba–Cl (118 kcal mol^{-1}) and Ba–O (134 kcal mol^{-1}), and was further supported by the FTIR spectrum of the nanoplate assemblies (Figure S3 in the Supporting Information). The energy-driven surface adsorption of OA molecules would then strengthen the ShDA and StDA effects of the surfactant mixtures, and thus lead to the formation of large-scale self-assemblies. Free-standing single-layered nanoplates (Figure 1e and f) could be obtained only when the organic micelle structures are distorted by partial removal of the capping ligands under refluxing or sonication in toluene during further disassembly procedures. In contrast, nanocrystals prepared in neat OM were smaller irregular nanoparticles without any ordered superstructures (Figure S4 in the Supporting Information).

In accordance with the TEM & HRTEM results, wide-angle XRD (WAXRD) patterns (Figure 2, top) confirm that the as-obtained BaFCl nanoplates form a pure tetragonal

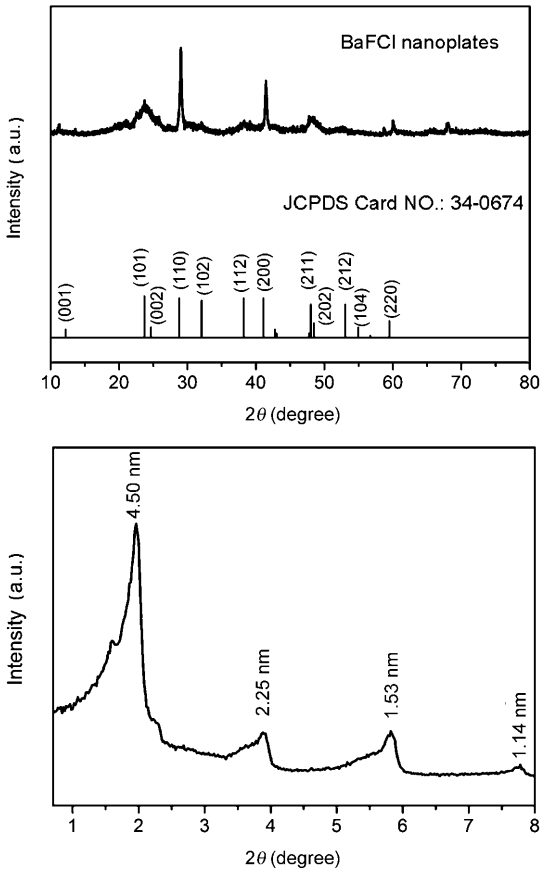

Figure 2. XRD characterization of superlattices of ultrathin BaFCl nanoplates. Top: WAXRD pattern of the BaFCl nanoplates prepared in the mixture of OA and OM and standard data for tetragonal BaFCl crystal (JCPDS Card No.: 34-0674). Bottom SAXRD pattern of the as-prepared superstructures with the peak labels of corresponding d spacings of the $00l$ ($l=1, 2, 3, 4.$) reflections.

structure (space group: *P4/nmm*), for which the 110 and 200 diffraction peaks are much sharper than those of the BaFCl nanoparticles (Figure S5), indicating the preferred growth in the XY plane to form large nanoplates in the matlockite structure. The direct formation of large-scale uniform 1D lamellar superstructures of these nanoplates in solution is further demonstrated by small-angle XRD (SAXRD) analysis performed on a dry membrane of the as-formed gel-like dispersion deposited on a glass wafer (Figure 2, bottom) as well as on the dried powders after being washed with cyclohexane and ethanol several times (Figure S6). The SAXRD pattern (Figure 2, bottom) of the as-deposited nanoplate films show four diffraction peaks with the 2θ angles of 1.96, 3.92, 5.82 and 7.78°. Thus, the corresponding d spacings are 4.5, 2.25, 1.53, 1.14 nm, which can be assigned to the $00l$ reflections of a lamellar mesostructure with the average periodic distance of about 4.53 nm, for which $l=1$, 2, 3 and 4,

respectively. The SAXRD results, in accordance with the TEM & HRTEM observations (Figure 1 and Figure S2 in the Supporting Information), reveal that the average distance between each neighboring nanoplate in the spontaneously self-assembled superstructures is just about 2 nm, suggesting the interplate-penetrating manner of the surface capping agents.

As shown in Scheme 1, an interfacial cooperation mechanism of both organic and inorganic species involved in the reaction was put forward to illustrate the spontaneous self-assembly of the domino-like BaFCl superlattices. In this scheme, the local stereochemical recognition match between the carboxyl groups of OA matrix and the Ba^{2+} ions in the inorganic crystal lattices at the organic–inorganic interface is considered as the key factor for this unusual ordered self-assembly of organic–inorganic hybrid mesostructures. At first, with the dissolution of $Ba(CX_3COO)_2$ (X = F, Cl) precursors in the mixed solution of OA and OM, metal–surfactant complex monomers combined with excess surfactant molecules and the exchanged CX_3COO^- species (which was confirmed by the FTIR spectrum of the precursor solution before taking decomposition, as shown in Figure S3 in the Supporting Information) would self-organize into layered mesostructures with alternate hydrophilic and hydrophobic layers, along with the release of Cl^- ions from the trichloroacetic groups upon heating to a certain temperature (Figure S7 in the Supporting Information). Then, in the presence of the Cl^- ions, self-assembled nuclei of BaFCl would be produced through the reaction of an ordered metal–surfactant complex with F^- ions released from the trifluoroacetic groups under elevated temperatures.[25] Afterwards, with the continuous diffusion of the metal–surfactant complex and halide anions into the as-formed mesostructures in the reaction solution, these self-assembled nuclei would gradually grow into domino-like superlattices of self-assembled crystalline nanoplates by means of face-to-face formation along the *c* axis, showing a significant shape-directing effect on single nanocrystals in the anisotropically layered tetragonal structure, together with a profound structure directing effect on the whole self-assembled mesostructures of the nanoplate–surfactant hybrid. Moreover, the whole highly compacted hybrid mesostructure would stay stable during the crystallization and growth procedure of the inorganic nanoplates, due to the stereochemical recognition match of the inorganic lattice and the organic micelle structure, as discussed hereafter.

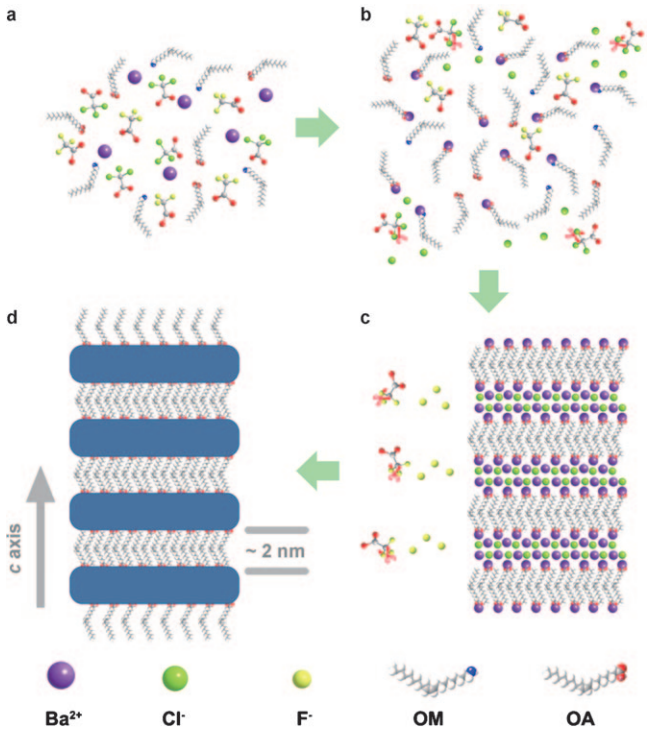

Scheme 1. Schematic presentation of the mechanism of the spontaneous self-assembly of nanoplates as an organic–inorganic cooperation model. a) Dissolution of $Ba(CX_3COO)_2$ (X = F, Cl) salts in OA/OM mixed solutions. b) Ligand exchange of Ba precursors and formation of metal–surfactant monomers. c) Formation of organic–inorganic hybrid layered mesostructures with different chemical species. d) Crystallization and growth of BaFCl nanoplates with the layered structures maintained.

A simple molecular mechanics model was established to identify the optimal configuration and steric energy of the assumed penetrated single-layered surface ligands adsorbed on the two face-to-face (001) facets of two neighboring BaFCl nanoplates (also see the modeling section in the Supporting Information). As shown in Figure 3a, a head-to-tail penetrated single layer of OA or stearic acid (SA, $C_{17}H_{35}COOH$) molecules was fixed between two neighboring tetragonal lattices with variable lattice constant. The stable configurations and conformations of a (2×3) lattice of the carbon chains of OA or SA were obtained by Monte Carlo method with the MMX force field when the inorganic lattice constant *a* varies from 350–600 pm. The steric energy curves (Figure 3d) of the carbon chains are both of a typical U shape, with the minimum energy point at about 440 pm for OA or at about 430 pm for SA. The computation results reveal that the constants of the most stable organic lattices of OA or SA match with that of the inorganic lattice of BaFCl ($a = 440$ pm) precisely, indicating that the assumed penetrated micelle structure is really stable in energy. Thus, the minimizing of both the surface energy of the inorganic nanoplates and the steric energy of the organic micelle structures would lead to the simultaneous formation and growth of the self-assembled organic–inorganic hybrid superstructures in solution.

A further time sequence experiment has verified the assumed interfacial cooperation model accounting for the formation of the domino-like BaFCl superlattices. A certain amount of the nanocrystals were extracted out from the reaction mixture by a syringe with a stainless steel needle every 5 min at the predetermined temperature (e.g., 300 °C). The structure and size of the as-prepared superlattices were then examined with TEM and dynamic light scattering (DLS) characterizations (Figure 4, Figures S8 and S9 in the Supporting Information). No nanoparticles or organic–inor-

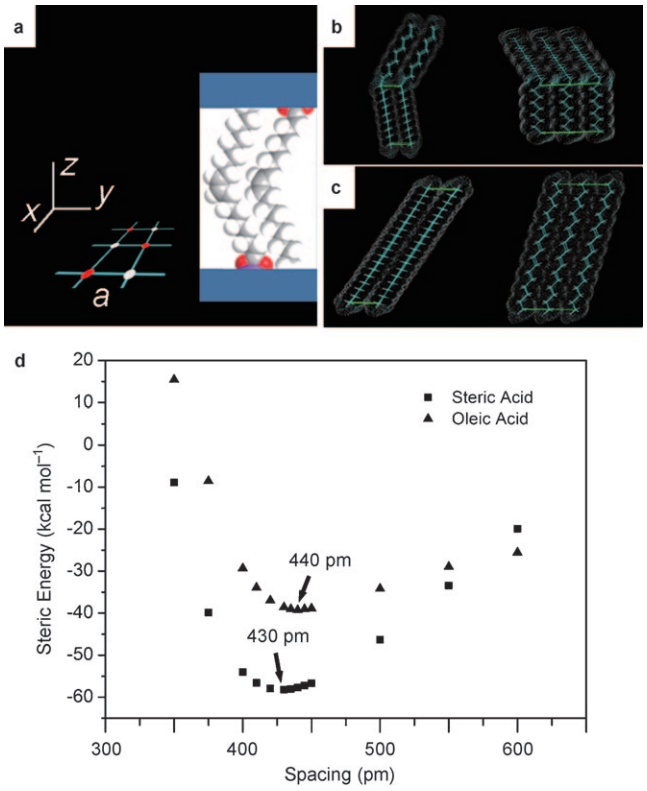

Figure 3. Molecular mechanics computation for a (2×3) lattice of penetrated single layer of OA or SA molecules adsorbed on two neighboring tetragonal lattice with a variable lattice constant. a) Schematic illustration for penetrated single layer of OA or SA. b) Calculated optimal configurations of OA molecules, from the *x* direction (left) and *y* direction (right). c) Calculated optimal configurations of SA molecules, from the *x* direction (left) and *y* direction (right). d) Calculated steric energy curve for the (2×3) lattice of penetrated single layer of OA or SA molecules.

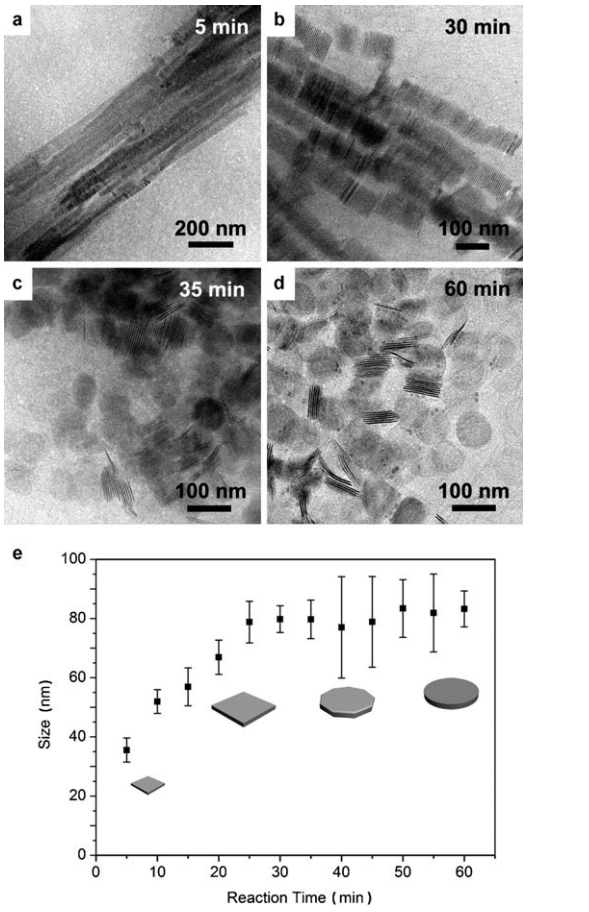

Figure 4. TEM observations of the as-prepared superstructres in a time sequence experiment: a) 5 min; b) 30 min; c) 35 min; d) 60 min. e) Size and shape evolution of the as-prepared BaFCl nanocrystals in the time sequence experiment (the particle sizes are counted from at least 50 nanocrystals).

ganic hybrid superstructures could be observed on the whole copper grid with the sample extracted at 0 min. Then, as the reaction solution turned white and turbid, plenty of long 1D self-assembled superstructures of ultrathin nanoplates (side length: ca. 35 nm) appeared in merely 5 min (Figure 4a) and then grew bigger in the next 20 to 25 min (Figure 4b and Figure S8a–d in the Supporting Information), as the thermolysis of the C–F bonds of the trifluoroacetic species is a continuous process, as supported by the TG-DTA analysis (Figure S7 in the Supporting Information). Furthermore, the DLS data (Figure S9 in the Supporting Information) revealed that large bundles of organic–inorganic superstructures were formed in the reaction solution through the above-described spontaneous process instead of an EISA protocol.[17] Then, after being heated in the following 30 min, these domino-like superstructures of the ultrathin nanoplates would gradually collapse into single-layered nanodisks (Figure 4c,d and Figure S8e and f in the Supporting Information) due to the possible thermal perturbation of the mesostructures. Meanwhile, rectangular nanoplates would also gradually transform into truncated rectangles or sub-rounded ones with wider size distributions (Figure 4d and Figure S8e and f in the Supporting Information), possibly due to the etching of the corners of the nanoplates and the spontaneous recrystallization process.[22] The size and shape evolution procedure of all these ultrathin building blocks are recorded in Figure 4e. In addition, some much smaller nanoparticles (10–20 nm in size), which appeared after 40 min (Figure 4d and Figure S8e and f in the Supporting Information) would possibly be generated by the collapse of ultrathin nanoplates, as proved by additional disassembly experiments of these superstructures implemented by refluxing or sonicating diluted dispersions of these superstructures in toluene (Figure S10a–c in the Supporting Information), indicating the stabilizing effects of the close-assembled structure for each thin layer of inorganic BaFCl nanoplates.

As predicted by the MM computation, any distortion of the "stable micelle structure" would result in the disruption of the domino-like hybrid superstructures. On the one hand, any distortions of the organic micelle structures would significantly hamper the formation of the stable, penetrated single layer of ordered surfactant molecules. Well-separated

single-layered BaFCl nanoplates or nanodisks (Figure S11 a–d in the Supporting Information) could be obtained by partially substituting the OA molecules with linear SA or lauric acid (LA) molecules without any further disassembly procedures. In addition, no long-term ordered, self-assembled superstructures, but separated nanoplates or nanotube-like nanostructures rolled from several nanosheets could be obtained in the mixed solution of SA or LA and OM due to the significant differences of molecular configurations between the linear carboxyl acid molecules (SA, LA) and the kinked OM molecules. On the other hand, ordered superlattices could be prepared in the mixed solution of SA and linear octadecylamine (ODA), or hexadecylamine (HDA), as shown in Figure S11e and f in the Supporting Information. In addition, as illustrated by the MM computation, the change of inorganic lattice would also prohibit the formation of ordered hybrid mesostructures or lead to the disruption of the layered mesostructures during the crystallization or growth procedure of inorganic nanocrystals. Instead, the assembly of nanocrystals would be realized in a "post-synthesis" way, producing superstructures with double-layered surface ligands between neighboring nanocrystals (4–5 nm in distance).[26] Further experiments proved that highly compacted and ordered domino-like superstructures of ultrathin SrFCl ($a=413$ pm) or BaFBr ($a=450$ pm) nanoplates could also be obtained (Figure S12a and b in the Supporting Information), while for CaFCl ($a=389$ pm) or Pr_2O_3 (cubic, $a=540$ pm) (Figure S12c and d in the Supporting Information), no robust domino-like superstructures could be obtained, since there is a mismatch of the inorganic and organic lattice. Instead, "post-synthesis" self-assembled superlattices with larger interplate distances (4–5 nm) are observed, due to the possible disruption of the micelle structure in the crystallization procedure of the inorganic phase.

In addition, by varying the molar ratio of the inorganic precursors and organic ligands, deferent kinds of self-assembled structures could be obtained. In the presence of an excess of surfactant, large uniform rectangular plates stacked in a tilting face-to-face way through a "post-synthesis" route could be observed (Figure S13a,b), since the solid hybrid structures could be disrupted by the addition of free surfactant molecules, leading to easy dispersion of the precursors in solution. In contrast, the decreasing the amount of free surfactant molecules resulted in highly compacted bamboo-like self-assembled superstructures with several ultra-large nanoplates (as two to five times larger than those "normal" ones) embedded into several nearby 1D chains (Figure S13c,d and Figure S14 in the Supporting Information).

In contrast to the unobservable fluorescence for the BaFCl bulk powder prepared through a co-precipitation-based hydrothermal method, the self-assembled BaFCl nanoplates showed an intense blue light in a wide peak centering at around 450 nm, when exited by a 360 nm UV light at room temperature (Figure 5). This broad photoluminescent band might result from the emissions of the intrinsic F centers, such as F(F^-), F(Cl^-), F(O^{2-}) and oxygen defects

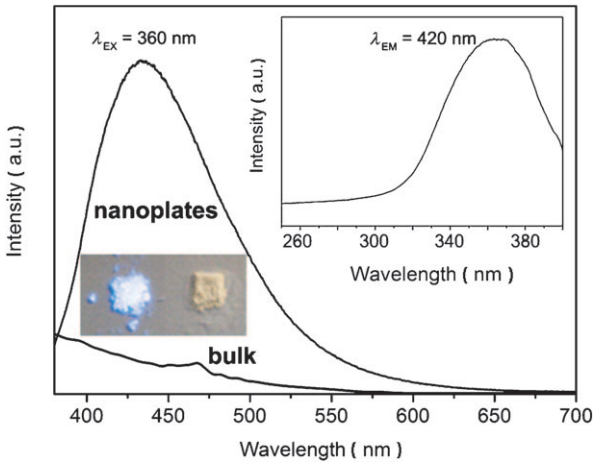

Figure 5. Fluorescence spectra of the self-assembled BaFCl nanoplates and the BaFCl bulk powder recorded at room temperature. Emission spectra ($\lambda_{ex}=360$ nm). Inset top right: excitation spectrum ($\lambda_{em}=420$ nm) of the nanoplates. Inset bottom left: digital image of the as-prepared self-assembled nanoplates (left) and the BaFCl bulk powder (right) under a portable lamp with 365 nm UV light.

(vacancies)[21] created in the superstructures during the one-step self-organization at the nanoscale.

In summary, robust fluorescent domino-like 1D superlattices of ultrathin nanoplates of alkaline earth halides were obtained in the solution phase without any artificial "post-synthesis" assembly. Supported by semiempirical molecular mechanics computation and practical experiment evidences, the stereochemical recognition match of various chemical species at the organic–inorganic interface (i.e., the fine lattice match of both the inorganic nanocrystals and the organic micelles) was demonstrated to account for the spontaneous self-assembly of the nanoplate superlattices in the solutions. This solution approach has demonstrated a conceptual advance for the construction of superlattice-based functional materials from diverse nano building blocks through novel biomimetic "bottom-up" strategies.

Experimental Section

Synthesis: A Schlenk line system was employed in the synthesis procedures. Oleic acid (OA; 90%, Aldrich), oleylamine (OM; > 80%, Acros), absolute ethanol, cyclohexane and toluene were used as received. In a typical synthesis, stoichiometric amounts of $Ba(CF_3COO)_2$ and of $Ba(CCl_3COO)_2$ (0.5 mmol) were dissolved in the solvent mixture of OA (4 mmol) and OM (36 mmol) in a three-necked flask at room temperature, degassed and heated to 140 °C with vigorous magnetic stirring for 15 min to remove water and other impurities with low boiling points. Next, the colorless, transparent solution was heated to 300 °C at a heating rate of 20 °C min^{-1} under a N_2 atmosphere. After 30 min of reaction, the white turbid solution was cooled to room temperature in air with gentle stirring for 5–10 min. Then the white gel-like products were separated by a centrifuge and washed several times with cyclohexane and ethanol, and dried at 80 °C for 12 h, showing a yield of ca. 80%.

Characterization: TEM observation was performed on a JEOL 2100 (JEOL, Japan) TEM operated at 200 kV. HRTEM and EDS analyses were conducted on a JEOL 2100F (JEOL, Japan) field emission TEM with EDS accessories operated at 200 kV. XRD patterns were obtained

with a Rigaku D/MAX-2000 diffractometer (Japan) using $Cu_{K\alpha}$ radiation ($\lambda = 154.06$ pm) with a slit of 1/2° at a scanning rate of 4° min^{-1} for wide-angle XRD characterizations, while a slit of 1/6° at a scanning rate of 1° min^{-1} were used for small-angle XRD measurements. FTIR spectra were determined on a Bruker Vector22 FTIR spectrometer. The DLS size distribution characterizations were done on a Horiba SZ-100 nano particle analyzer (Horiba, Japan). UV-simulated photoluminescence properties were measured on a Hitachi F-4500 fluorescence spectrophotometer (Hitachi, Japan) with a Xenon lamp as a stimulation source. The scanning speed was fixed at 60 nm min^{-1} with both the excitation and emission splits fixed at 2.5 nm.

Acknowledgements

This work was supported by the NSFC (grant nos. 21025101, 20871006, and 20821091) and by MOST of China (grant No. 2011AA03A407). Y.W.Z. particularly appreciates the financial aid of China National Funds for Distinguished Young Scientists from the NSFC.

Keywords: alkaline earth metals · halides · molecular recognition · nanostructures · self-assembly · superstructures

[1] G. M. Whitesides, B. Grzybowski, *Science* **2002**, *295*, 2418–2421.
[2] J. Aizenberg, *MRS Bull.* **2010**, *35*, 323–330.
[3] R. F. Service, *Science* **2005**, *309*, 95–95.
[4] Z. Y. Tang, N. A. Kotov, S. Magonov, B. Ozturk, *Nat. Mater.* **2003**, *2*, 413–418.
[5] E. V. Shevchenko, D. V. Talapin, N. A. Kotov, S. O'Brien, C. B. Murray, *Nature* **2006**, *439*, 55–59.
[6] D. V. Talapin, E. V. Shevchenko, M. I. Bodnarchuk, X. C. Ye, J. Chen, C. B. Murray, *Nature* **2009**, *461*, 964–967.
[7] S. M. Rupich, E. V. Shevchenko, M. I. Bodnarchuk, B. Lee, D. V. Talapin, *J. Am. Chem. Soc.* **2010**, *132*, 289–296.
[8] D. V. Talapin, J. S. Lee, M. V. Kovalenko, E. V. Shevchenko, *Chem. Rev.* **2010**, *110*, 389–458.
[9] A. G. Dong, J. Chen, P. M. Vora, J. M. Kikkawa, C. B. Murray, *Nature* **2010**, *466*, 474–477.
[10] J. H. Yu, X. Y. Liu, K. E. Kweon, J. Joo, J. Park, K.-T. Ko, D. W. Lee, S. P. Shen, K. Tivakornsasithorn, J. S. Son, J.-H. Park, Y.-W. Kim, G. S. Hwang, M. Dobrowolska, J. K. Furdyna, Taeghwan Hyeon, *Nat. Mater.* **2010**, *9*, 47–53.
[11] F. Kim, S. Kwan, J. Akana, P. D. Yang, *J. Am. Chem. Soc.* **2001**, *123*, 4360–4361.
[12] E. V. Shevchenko, D. V. Talapin, C. B. Murray, S. O'Brien, *J. Am. Chem. Soc.* **2006**, *128*, 3620–3637.
[13] T. P. Bigioni, X. M. Lin, T. T. Nguyen, E. I. Corwin, T. A. Witten, H. M. Jaeger, *Nat. Mater.* **2006**, *5*, 265–270.
[14] J. Aizenberg, A. J. Black, G. M. Whitesides, *Nature* **1998**, *394*, 868–871.
[15] J. Aizenberg, A. J. Black, G. H. Whitesides, *J. Am. Chem. Soc.* **1999**, *121*, 4500–4509.
[16] J. Aizenberg, A. J. Black, G. H. Whitesides, *Nature* **1999**, *398*, 495–498.
[17] M. Li, H. Schnablegger, S. Mann, *Nature* **1999**, *402*, 393–395.
[18] H. Cölfen, S. Mann, *Angew. Chem.* **2003**, *115*, 2452–2468; *Angew. Chem. Int. Ed.* **2003**, *42*, 2350–2365.
[19] H. Cölfen, M. Antonietti, *Angew. Chem.* **2005**, *117*, 5714–5730; *Angew. Chem. Int. Ed.* **2005**, *44*, 5576–5591.
[20] T. Xie, S. A. Li, W. B. Wang, Q. Peng, Y. D. Li, *Chem. Eur. J.* **2008**, *14*, 9730–9735.
[21] W. Chen, N. Kristianpoller, A. Shmilevich, D. Weiss, R. Chen, M. Z. Su, *J. Phys. Chem. B* **2005**, *109*, 11505–11511.
[22] Y. Yin, A. P. Alivisatos, *Nature* **2005**, *437*, 664–670.
[23] A. Firouzi, D. Kumar, L. M. Bull, T. Besier, P. Sieger, Q. Hou, S. A. Walker, J. A. Zsadzinski, C. Glinka, J. Nicol, D. Margolese, G. D. Stucky, B. F. Chmelka, *Science* **1995**, *267*, 1138–1143.
[24] P. D. Yang, D. Y. Zhao, D. I. Margolese, B. F. Chmelka, G. D. Stucky, *Nature* **1998**, *396*, 152–155.
[25] Y. W. Zhang, X. Sun, R. Si, L. P. You, C. H. Yan, *J. Am. Chem. Soc.* **2005**, *127*, 3260–3261.
[26] Z. Y. Huo, C.-K. Tsung, W. Y. Huang, M. Fardy, R. X. Yan, X. F. Zhang, Y. D. Li, P. D. Yang, *Nano Lett.* **2009**, *9*, 1260–1264.

Received: April 1, 2011
Published online: June 3, 2011

